Proceedings of the 1st Global Power and Propulsion Forum
GPPF 2017
Jan 16-18, 2017, Zurich, Switzerland
www.pps.global

GPPF-2017-91

A simplified method for wall temperature prediction in externally cooled turbines

R. Poli
TU Delft
Delft, The Netherlands
R.Poli@student.tudelft.nl

M. Pini
TU Delft
Delft, The Netherlands
M.Pini@tudelft.nl

A. G. Rao
TU Delft
Delft, The Netherlands
A.GangoliRao@tudelft.nl

The article presents a new procedure to calculate the wall temperature of film-cooled turbine blades. The methodology utilises semi-empirical relations for film cooling effectiveness developed for a flat plate. The correlations are corrected a-posteriori with parameters (Mach number, pressure, etc) resulting from aerodynamic analysis, performed by means of the Multiple Blade Interacting Streamtube Euler Solver (MISES). With the proposed approach, the disadvantages of the classical 2D approaches, that deal with slots instead of film cooling holes, are circumvented. The procedure is validated against experimental data and 3D CFD results. It is shown that the method, despite its simplicity, is relatively accurate and computationally efficient, the computational cost being an order of magnitude lower than that of the conventional approaches. Thanks to this, the methodology is suited for Multidisciplinary Design Optimisation (MDO) problems involving the conceptual aerothermo-structural design of turbine blades.

1 Introduction

Despite the ever increasing computational resources and the development of new, reliable numerical models for CFD, 3D fluid-dynamic simulations of externally cooled turbine blades are excessively demanding to be integrated in a Multidisciplinary Design Optimisation (MDO) frameworks. The possibility to account for different design aspects (e.g. aerodynamics, structure, heat transfer) with integrated high-fidelity tools usually makes MDO well suited for detailed design of gas turbine blades, but rarely applicable in their conceptual design phase. To address this issue, a simplified method for wall temperature prediction of externally cooled turbine blades suitable for conceptual design, is developed, described and discussed here.

Accurately predicting the surface temperature of a turbine blade in the design phase is essential because the creep life of a component exponentially decreases with the operating temperature, in these applications. In fact, modern turbine blades can operate at gas temperatures well above their melting point temperature, and only an advanced cooling system can guarantee their operations. Therefore, aerodynamic design must be supplemented by thermal and thermally-induced stress analysis to achieve efficient and lasting blade configurations. This is the focus of MDO approaches for gas turbine blades.

The first milestone in the field of MDO of externally cooled blades was accomplished by Haendler et al [1]. They studied a first-stage High Pressure Turbine (HPT) blade of an engine for terrestrial application, both numerically and experimentally. The numerical models were simplified as much as possible: bi-dimensional aerodynamic computations at various spanwise locations with $k-\varepsilon$ turbulence model and with slots (instead of holes) whose boundary conditions were specified according to the work of Rodi et al [2] to partly consider the 3D effects. Despite the simplifying assumptions, the study showed a fairly good agreement between the results from the simplified numerical problem and the experimentally tested set-up (differences of $\approx 10\%$).

In 1998, Talya et al began some MDO studies that can be found in four consecutive papers, [3], [4], [5] and [6].

Despite the differences in the problem formulation among the various papers, the external aerodynamics was always studied with the 2D numerical code RVCQ3D. Film cooling effects were partly included: boundary conditions were adjusted on the blade surface to take into account the exit of relatively cold air. In practice, Talya simulated slots, which are more efficient than discrete holes but are not feasible in realistic applications.

Mousavi et al [7] tackled the problem by means of a 2D solver based on the 0-equation turbulence model by Baldwin-Lomax. It is proved to be fast and partly reliable for high subsonic M, but is limited by the representation of the cooling holes as slots. The resulting temperature of the surface is under-predicted. The advantage is that it takes into account the losses due to the injection of cold air.

More recent studies such as those by Song et al [8] and Chi et al [9], have tried to integrate 3D CFD simulation in their MDO framework, at the expense of reducing the number of variables to around 10, thus limiting design flexibility, and using a gradient-based algorithm to reduce the computational time (which was still between 1 and 2 months).

The limits of traditional 2D approaches studying slots become evident by means of the following example. Figure 1 presents two cases where the same boundary conditions are applied: blowing ratio $M = (\rho_c V_c)/(\rho_\infty V_\infty) = 1$ and density ratio $DR = \rho_c/\rho_\infty = 2$, on a flat plate with a single row of holes with a diameter $D = 1mm$. The only difference is that in one case a cylindrical hole is studied in 3D, while in the second case only the symmetry plane of the problem is simulated. In this 2D case, the coolant remains attached to the target surface for a longer distance because of the absence of the kidney vortices.

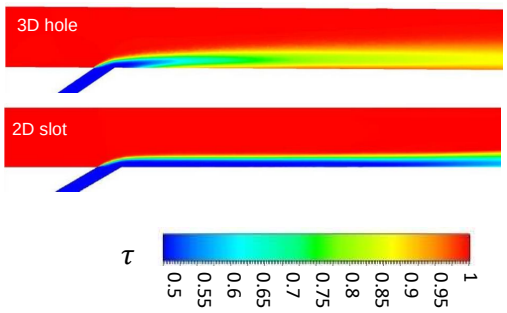

Fig. 1. Contours of normalised fluid temperature ($\tau = T/T_{0,in}$) for a 2D slot and a 3D hole with the same injection angle and operating conditions

Based on these considerations, a new method for wall temperature prediction is proposed, validated and discussed. More specifically, the surface temperature of the blade is calculated by means of semi-empirical correlations developed for a flat plate, that are corrected with the local flow properties; these corrections are calculated with an aerodynamic analysis of the same blade in which external cooling is neglected. Therefore, the procedure still necessitates of 2D aerodynamic analyses, but accounts for the actual effect of holes through well-established correlations. Conversely, in classical approaches only span-wise sections of the 3D blade are considered and simulated, see [10], [11], etc. The cutting radii are chosen such that the film cooling holes are included in the domain. In this way, the inherent disadvantage is that the method approximates the holes as cooling slots, neglecting the complex interaction between the coolant and the mainstream. Eventually, the simulated problem is significantly different from the real one, as observed in Fig. 1.

This procedure is proved to be accurate enough for engineering calculations and less computationally expensive as compared to existing approaches. As a result, it is highly suited to be included as analysis tool in optimization problems in which the blade metal temperature must be minimized while enhancing the fluid-dynamic performance of the cascade.

The paper is structured as follows: at first, in Section 2, the methodology is presented, then the method is applied to realistic geometries and validated against experimental and numerical data coming from RANS analyses, Sections 3 and 4. Finally, Section 5 presents the conclusions, showing advantages and limitations of the present approach.

2 Methodology

The rationale of the new procedure, which is referred to as Corrected film Cooling Correlations method, or C^3, is to compute the effects of film cooling by means of semi-empirical relations once obtained the temperature distribution of an uncooled blade through adiabatic aerodynamic analysis. Figure 2 shows the schematic of the method.

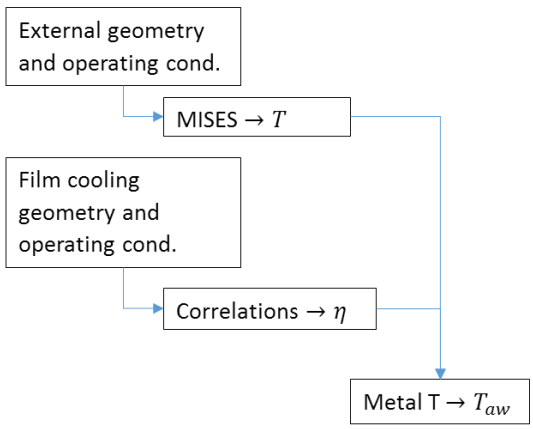

Fig. 2. Logic scheme of the C^3 method

More in detail, the objective is to estimate the adiabatic wall temperature T_{aw}, which is retrieved from the definition of the film cooling effectiveness η, that is:

$$\eta = \frac{T - T_{aw}}{T - T_c} \tag{1}$$

where T_c is the coolant temperature at the exit of the hole, T is the adiabatic flow static temperature and η the cooling effectiveness. In particular, the effectiveness is calculated with the correlation for cylindrical holes of Baldauf et al [12], which is one of the most widely used in literature due to the broad set of variables tested in the experiments and the accuracy of the formula in an engine-like representative domain. Eq. 2 expresses the laterally averaged film cooling effectiveness:

$$\overline{\eta} = \eta_c \frac{DR^{0.9D/s}}{(\sin(\alpha))^{0.06s/D}} \tag{2}$$

where DR is the density ratio, s/D the spanwise spacing, α the injection angle and η_c a factor that depends on the turbulence level and other geometrical and physical properties. Further details can be found in [12]. For multiple rows of holes, Eq. 3 by Sellers is used (as already done by Mehandale, Bogard and Bradley [13]):

$$\overline{\eta_{tot}} = \overline{\eta_1} + (1-\overline{\eta_1})\overline{\eta_2} + ... + (1-\overline{\eta_1})...(1-\overline{\eta_{N-1}})\overline{\eta_N} \tag{3}$$

It can be seen that Eq. 3 accounts for the interaction between consecutive rows of holes, whose effectiveness $\overline{\eta_1}$, $\overline{\eta_2}$, ..., $\overline{\eta_N}$ can be calculated with Eq. 1.

The second input of Eq. 1, the static temperature T, is calculated by means of Eq. 4.

$$\frac{T_0(x)}{T(x)} = 1 + \frac{\gamma - 1}{2} M(x)^2 \tag{4}$$

where the subscript $_0$ refers to the total property and x is the stream-wise coordinate. In this work, the static temperature distribution on the blade surface is calculated by viscous aerodynamic analysis performed by the numerical code MISES (Multiple Blade Interacting Streamtube Euler Solver) and M is taken on top of the Boundary Layer. The tool was developed by Drela and Youngren of MIT [14]. MISES has been used in the past by various groups of research, as summarised by Andrew [15], to study and optimise turbomachines through 2D analyses. The execution of the code was automated by means of MATLAB.

The inherent disadvantage of C^3 is connected to the impossibility to physically model the interaction between the coolant and the mainstream and thus it could have problems in those regions when the interaction is significant (boundary layer separation due to film cooling, etc.). To alleviate these issues, transition of the boundary layer is imposed in MISES at the location of the first row of holes, an assumption that is based on the work by Al Zurfi et al [16], where the Large Eddy Simulations (LES) showed that the coolant which is ejected from the holes locally increases the turbulence level and thus the possibility of transition. All the other interactions between the coolant and the main flow are neglected.

The mentioned procedure is valid for externally cooled geometries whereas for non-cooled blades, or in regions upstream of the first row of cooling holes, Eq. 5 applies:

$$T_{aw} = T_s \left(1 + r \frac{\gamma - 1}{2} M^2\right) \tag{5}$$

where r is the recovery factor that depends on the flow properties and in particular on its regime: for laminar flows it is assumed to be $r = \sqrt{Pr}$, for turbulent ones $r = \sqrt[3]{Pr}$.

Finally, for non-adiabatic cases, an additional equation is needed to retrieve the metal temperature from T_{aw}. Two semi-empirical correlations by Wang et al in 2006 [17] in terms of average Nu are used for this purpose. Equations 6 and 7 refer to $Re \leq 10^5$ and $Re \geq 5 \cdot 10^5$, respectively. For intermediate values, linear interpolation is applied.

$$Nu = 2.483 Re^{0.389} Pr^{1/3} \tag{6}$$

$$Nu = 0.0943 Re^{0.636} Pr^{1/3} \tag{7}$$

3 Validation and Verification of the C^3 method

The verification and validation of the C^3 method is approached in two-steps: at first, MISES is compared to experimental data (the LS89 nozzle guide vane, [18]) to assess the accuracy of the simulation tool; then, the proposed methodology is validated against two sets of experimental data (the NASA Energy Efficient Engine, stages 1 and 2 of the HPT, and two test cases studied by Haller et al [10]) and against some other geometries also studied with a computationally more expensive method. In this case 3D RANS CFD is used for comparison.

3.1 Verification of MISES

The test case was the LS89 nozzle guide vane studied in the 1990s by Prof. Toni Arts at the Von Karman Institute for Fluid Dynamics [18]. The same configuration was tested with a RANS CFD approach (using ANSYS CFX 16.1) to

compare MISES with RANS. In particular, two different methods were used in CFX: inviscid calculation and simulation with a Shear Stress Transport (SST) $k-\omega$ turbulence model. The same mesh, consisting of around $120k$ cells with an average $y_+ \approx 1$, was used. The steady-state, 3D, single-phase, compressible simulations required 3 to 11 minutes, depending on the type of analysis and on 6 cores (Intel®Core™ i7-4700HQ). The periodicity condition was applied to decrease the domain size and therefore the computational time.

The MISES analyses were run with a mesh of $\approx 25k$ cells and took less than 2 minutes on a single processor. A detail of the 2D mesh can be seen in Fig. 3.

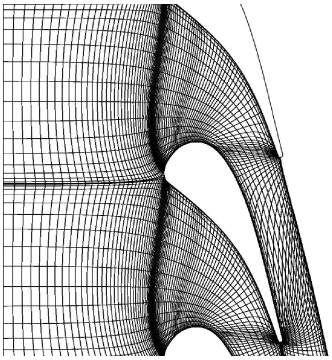

Fig. 3. LS89: detail of the MISES mesh

The results for the two cases, $M_{is,out} = 0.875$ and 1.020, are expressed in terms of the isentropic Mach number, defined as:

$$M_{is} = \sqrt{\frac{2}{\gamma - 1}\left[\left(\frac{P_{0,in}}{P}\right)^{\frac{\gamma-1}{\gamma}} - 1\right]} \tag{8}$$

where P is the static pressure on the blade surface. The experimental and numerical data can be seen in Fig. 4 where the M_{is} on the upper and lower surfaces are depicted as function of the curvilinear abscissa s. Results refers to the case with $Tu = 3\%$ and an averaged isentropic Mach at the outlet $M_{is,out}$=0.875 and 1.020.

The numerical calculation correlates well with the experimental data. All the simulations have shock-capturing capabilities and the pressure profile along the blade is always captured with a maximum deviation of around 5%.

Quite accurate predictions were found also for inviscid calculations, which was carried out to be compared to a coupled viscous/inviscid one in terms of computational time and M_{is}. It turned out that MISES is faster than CFX, mainly because of the denser mesh in the second case.

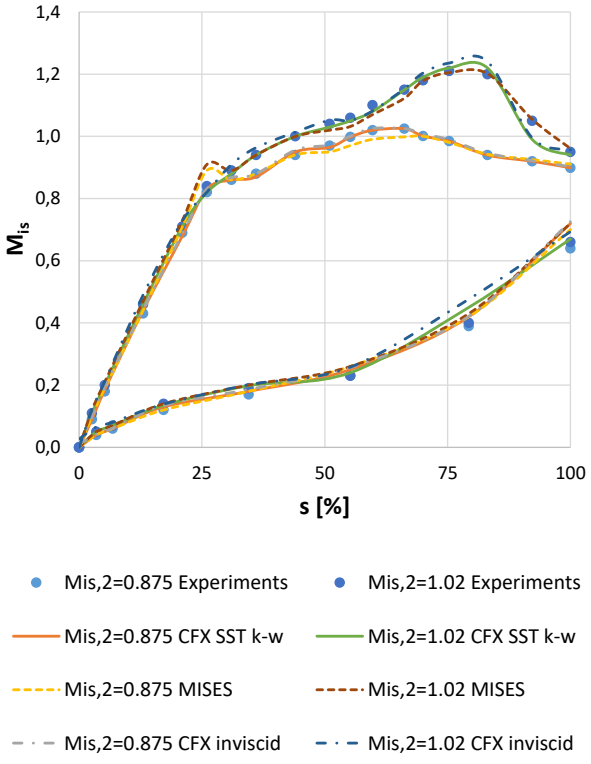

Fig. 4. MISES validation: LS89 experimental and numerical results in terms of M_{is}

As far as the heat transfer is concerned, a comparison between the predicted and the measured heat transfer coefficients was carried out. In this case only ANSYS CFX was used since the same set-up will be then used to validate the new approach. The tested case has the following operating parameters: $Tu = 1\%$, $Re = 2E+06$ and $M_{is,out} = 1.090$. Results are shown in Fig. 5 and show an overall good agreement, except at the stagnation point where the fully turbulent model cannot properly predict laminar boundary layer and its transition.

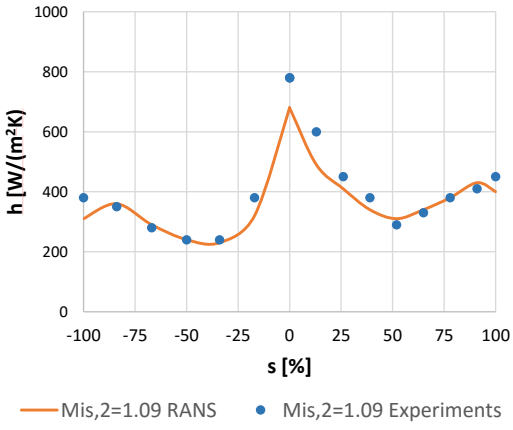

Fig. 5. RANS validation: LS89 experimental and numerical results in terms of heat transfer coefficient

Further validation studies were not performed due to the abundant material already existing in literature, which has been summarised and extended by Andrew in [15].

So far, the positive aspects of MISES have been shown. However, two main problems, already known in literature, were addressed and must be known to the reader:

- **Convergence issues in transonic cases.** The first problem is that the numerical code can experience a significant increase in the computational time (up to 10 times) or divergence in transonic and supersonic cases. The phenomenon is hard to cure since it is difficult to be predicted. The modification of dedicated parameters can however avoid these issues in most of the cases. These parameters are the critical Mach number M_{crit} (as it is defined in the bulk viscosity) and the artificial dissipation coefficient C_μ. They both appear in the formulation of the first order dissipation coefficient μ_i^1, Eq. 9, a factor which has been introduced in CFD to promote stability and shock-capturing capabilities.

$$\mu_i^1 = \frac{C_\mu}{\gamma}(1-M_{crit})\left(1+exp\left(\frac{1+1/M^2}{1-M_{crit}}\right)\right) \qquad (9)$$

  Recommended values for transonic cases are $M_{crit} = 0.95$ and $C_\mu = 1.2$. Despite these corrections to the original model, some cases still diverge, showing the need for more robust set-ups. In fact, in the recent years, time-marching methods have been developed despite their increased computational costs and are usually implemented in the commercial CFD tools because they are more stable.

- **Poor prediction of the fluid physics of the blunt trailing edges.** The problems depend on the direct specification of the Kutta condition at the trailing edge instead of properly and explicitly modelling the flow physics. In particular, the code applies the condition in a point that the user has to specify: while this is obvious in a sharp profile, it is hard to predict a-priori which point is the one the Kutta condition has to be applied to. An example of what happens if such a point is wrongly specified can be found in Fig. 6: it can be seen that this error results in a very small radius of curvature the flow has to follow, and thus extremely high local velocity (hypersonic, in this case).

  Andrews arrived to the same conclusions in his validation studies [15]:

  > *An inherent disadvantage of this modelling approach is that it under-predicts losses arising in the wake region, and, relatedly, it does not predict base pressure at the trailing edge.*

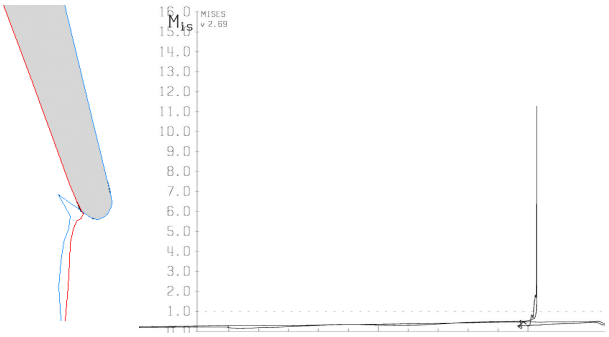

Fig. 6. LS89 blunt trailing edge: example of the wrong specification of the point where the Kutta condition is applied

  Two possible solutions were elaborated: the first one would be to run various cases representing the same geometry but with different location of the point where Kutta-condition is applied until a solution without local super-velocities is found; the second one is to study only profiles with sharp trailing edges. Despite the second solution excludes some possible geometries from the design space, it guarantees robustness and it is easily automated since no human correction on the point where the Kutta condition is specified is needed.

Despite the mentioned disadvantages that could harm the robustness of the procedure, MISES was proved to be a valuable tool that is suitable for rapid and accurate analysis of turbine cascades.

4 Results and Discussion

The C^3 method was applied to estimate the blade metal temperature in four different flow problems, namely:

- A symmetric aerofoil (NACA 0012) at zero incidence angle and with 2 rows of in-line film cooling holes on each side.
- NACA 0012 with 2 rows of staggered film cooling holes on each side. A qualitative comparison of the first two cases can be seen in Fig. 7.
- A Nozzle Guide Vane (NGV) with two different streamwise location of film cooling holes, from the experiments by Haller et al [10].
- HPT stages 1 and 2 of the NASA Energy Efficient Engine, [19] and [20].

As far as the MISES setup is concerned, the default mesh properties were used and M_{crit} and C_μ were set to 0.95 and 1.2, respectively. Results will be presented in the form of span-wise averaged wall temperature, normalized with respect to the total inlet temperature:

$$\tau = \frac{T_w}{T_{0,in}} \qquad (10)$$

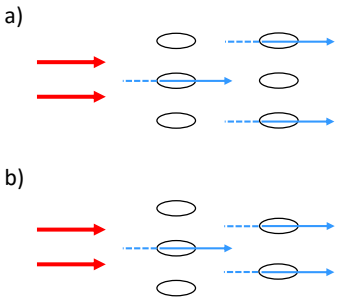

Fig. 7. Qualitative comparison of inline (a) and staggered (b) configurations. Red arrows are for mainstream, blue for the coolant

4.1 NACA 0012 in-line

The first case to be studied was a NACA 0012 profile at zero incidence angle with 2 rows of in-line film cooling holes on each side at 4% and 22% of the chord respectively, Fig. 8. Due to symmetry, only one side was included in the domain.

Fig. 8. Lateral view of NACA 0012 profile with film cooling holes.

The same CFD settings as before were used for the 3D analysis and the operating conditions were: $\alpha = 25°$, $\theta = 0°$, $D_h = 1mm$, $s/D_h = 4$, $DR = 2$ and $M = 1$.

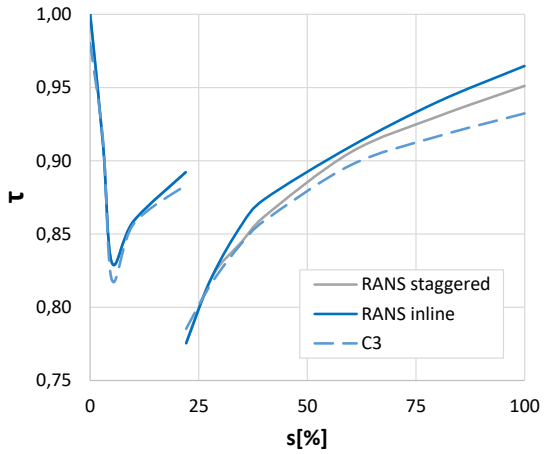

Fig. 9. NACA 0012 with inline and staggered cooling holes. τ as a function of s.

Results are shown in Fig. 9. It can be noticed that the deviations with respect to 2D CFD is within 3%. The region where this error is higher is close to the trailing edge. Further explanations of this difference will be discussed in the later sections. The computational time required by C^3 to calculate the wall temperature was $51s$.

4.2 NACA 0012 staggered

The same case as before (same operating conditions and computational settings) was tested but with staggered rows. Also in this case the maximum error is within 3% and once again it is more pronounced in the trailing-edge region. A possible explanation is connected to the formation of kidney vortices, which induce the mixing of the coolant with the hot gases, thus decreasing the performance of the cooling system. According to the results, the C^3 method is able to capture the trend of temperature in stream-wise direction rather accurately. In this context, another study was carried out: a comparison between an in-line arrangement and a staggered one with the same boundary conditions. This difference cannot be captured by the correlations, which then presents the same results in the two cases. Also CFD apparently present similar results for these two different cases, Fig. 9. The reason is the averaging of the temperature in span-wise direction that hides the real physics of the problem, presented in Fig. 10 for the two cases studied above: NACA 0012 aerofoil with in-line and staggered holes.

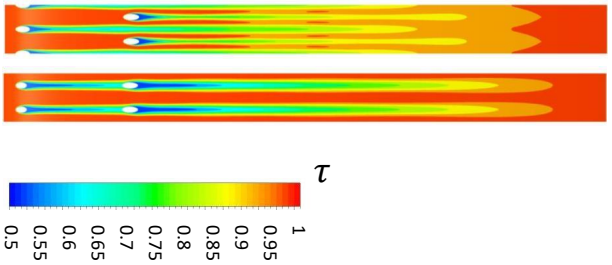

Fig. 10. NACA 0012 staggered and in-line holes: comparison of normalised wall temperature.

As it can be seen, the variations of temperature in the spanwise direction is larger for the in-line holes as compared to the staggered configuration. This configuration is usually preferred in realistic application because the strong non uniformity of temperature of in-line arrays causes local hot spots and thermal stresses, which are not beneficial for creep life. Furthermore, since the coverage is more uniform in this case, the correlations give a more precise description of the flow physics because they average the properties (that are almost constant also in the CFD solution) in spanwise direction.

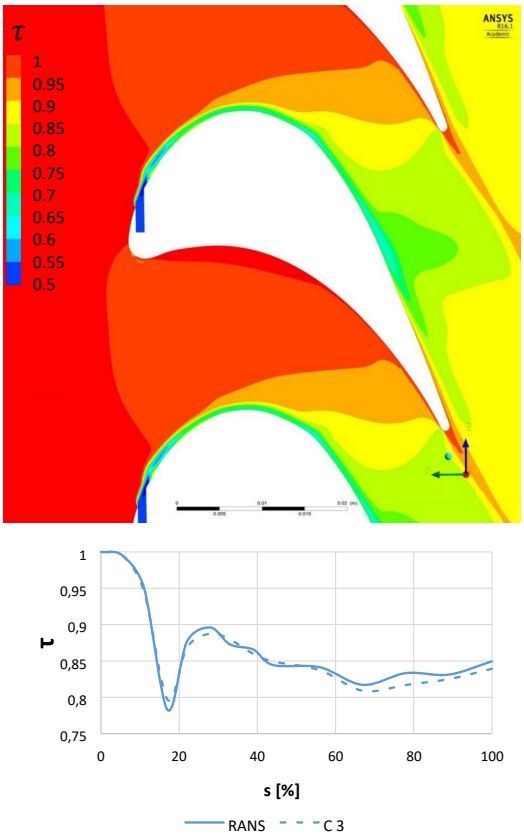

Fig. 11. Case NGV 1: contours of normalised temperature from RANS (top) and τ comparison between RANS and C^3 (bottom)

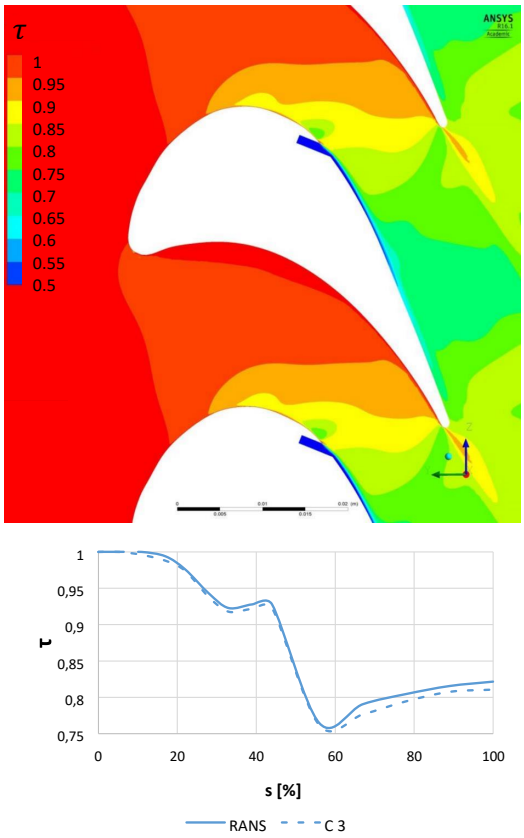

Fig. 12. Case NGV 2: contours of normalised temperature from RANS (top) and τ comparison between RANS and C^3 (bottom)

4.3 A transonic Nozzle Guide Vane

After the preliminary studies presented so far, C^3 was tested against a more realistic case: a transonic Nozzle Guide Vane (NGV) experimentally studied by Haller et al [10]. The same blade geometry as in the experiments was simulated and two relevant (among the five) hole locations were chosen: a case where the hole is placed in an accelerating flow field (Case NGV 1) and a case where the hole location is in a diffusing region (Case NGV 2). The blowing ratio of $M = 1$ was chosen, as in the experiments. The cases were studied both with the already validated RANS setup and with C^3. Periodic boundary conditions were specified in CFX to reduce the domain size and therefore the computational time. The results are expressed in terms of the laterally averaged adiabatic wall temperature, shown in Fig. 11 and 12. In both cases the deviations are below 2%, confirming that C^3 method features similar accuracy than CFD even in realistic configurations. The upper parts of the figures show the contours of air static temperature coming from a 3D simulation. In both cases the coolant remains attached to the blade, thus resulting in the relatively low wall temperatures also captured by C^3.

A comparison between the proposed approach and RANS in terms of computational time is presented in table 1. All the calculations were run on a Intel®Core™ i7 CPU.

Table 1. Computational time. A comparison between the classic RANS approaches in 2D and C^3

Case	RANS	C^3
NACA 0012 inline	627 s	51 s
NACA 0012 staggered	701 s	51 s
NGV	973 s	108 s
NASA E^3	-	142 s

4.4 NASA EEE HPT stages 1 and 2

The last validation study was performed for the HPT stages 1 and 2 of the NASA Energy Efficient Engine, experimentally investigated by NASA researchers in [19] and [20], Fig. 13.

The cooling system comprises 6 rows of holes in HPT stage 1 and 2 rows in stage 2. The results are reported in Fig. 14.

A maximum deviation of 3% with respect to experiments was observed in the results, demonstrating the capability of the proposed method in more complex cooling system arrangements. In particular, the main differences can be seen in the trailing-edge region, that is by far unresolved by vis-

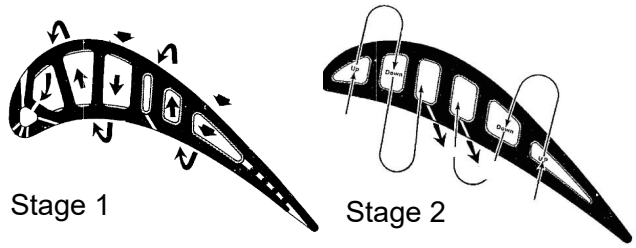

Fig. 13. NASA Energy Efficient Engine, HPT: stage 1 (left) and stage 2 (right)

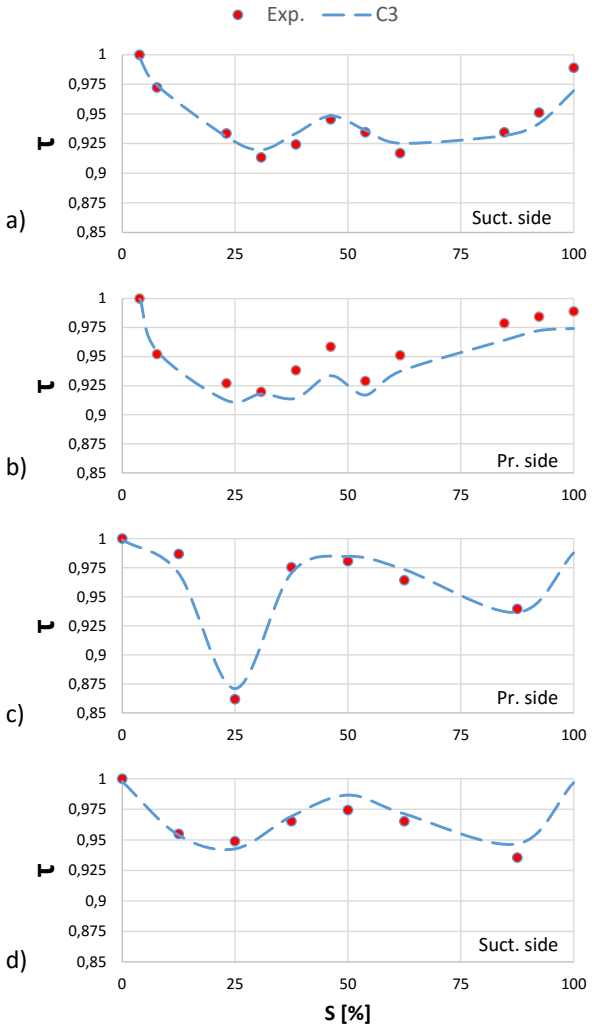

Fig. 14. NASA Energy Efficient Engine, HPT: surface temperature (predicted and measured) of stages 1 (a,b) and 2 (c,d), suction and pressure sides

cous aerodynamic solvers, and in the pressure side of stage 1, where 5 holes are present and the temperature is under-predicted. In this case, the discrepancies could be associated to the intrinsic limitation of Eq. 3 in modelling multiple rows of holes.

5 Conclusions

In the paper, a new method to predict the film cooling performance in terms of wall temperature has been developed and validated. The method has been proved to have several advantages:

- It is **computationally efficient**, since the usually employed 3D CFD analyses are one order of magnitude computationally more demanding.
- The approach is relatively accurate even in complex applications. The typical maximum deviation is found to be less than $< 3\%$ if compared to experimental or 3D CFD results.

Thanks to these features, it is deemed particularly attractive for conceptual design purposes in automated MDO algorithms.

Possible inaccuracies, and in particular under-prediction of wall temperature, may arise when the interaction between the coolant and the mainstream cannot be neglected:

- Increase in turbulence downstream of the cooling hole due to the kidney vortices is not fully captured, thus resulting in a small over-prediction of the cooling system performance in the trailing edge regions.
- Multiple rows of holes (> 3 rows) are not properly modelled, probably due to a limited applicability of Eq. 3.
- Local super-velocities, regions of low speed and local boundary layer separation triggered by the coolant and mainstream interaction cannot be captured due to inherent limitations of the methodology.

To summarise, the proposed method has been demonstrated to be suitable for systematic heat transfer analysis in the preliminary design phase of the high pressure turbines.

Nomenclature

Symbols

C_μ Artificial dissipation coefficient [-]
D Hole diameter [m]
DR Density ratio [-]
h Heat transfer coefficient [W/(m^2K)]
k Turbulent kinetic energy [J/kg]
M Blowing ratio [-] or Mach number [-]
Nu Nusselt number [-]
P Pressure [Pa]
Pr Prandtl number [-]
r Recovery factor [-]
Re Reynolds number [-]
s Spanwise coordinate [m]
T Temperature [K or °C]
Tu Turbulence intensity [%]

x Streamwise coordinate [m]

Greek letters

α Injection angle [deg]
γ Heat capacity ratio [-]
ε Turbulent dissipation [J/(kg s)]
η Film cooling effectiveness [-]
μ_i^1 First order dissipation coefficient [-]
τ Dimensionless temperature
ω Specific turbulence dissipation rate [1/s]

Subscripts

0 Total property
aw Adiabatic wall
c Coolant
in Property at inlet
is Isentropic
out Property at outlet

Acronyms

C^3 Corrected film Cooling Correlations
CFD Computational Fluid Dynamics
HPT High Pressure Turbine
NGV Nozzle Guide Vane Design Optimisation
MDO Multidisciplinary Design Optimisation
RANS Reynolds Averaged Navier-Stokes equations

References

[1] Haendler, M., Raake, D., and Scheurlen, M., 1997. "Aero-thermal design and testing of advanced turbine blades". *ASME Conference Proceedings*.

[2] Rodi, W., 1992. "The Influence of Density Difference Between Hot and Coolant Gas on Film Cooling by a Row of Holes : Predictions and Experiments". *Journal of Turbomachinery,* **114**(October 1992), pp. 747–755.

[3] Talya, S. S., Rajadas, J. N., and Chattopadhyay, A., 1998. "Multidisciplinary Design Optimization of Film-Cooled Gas Turbine Blades". *Mathematical Problems in Engineering,* **5**, pp. 97–119.

[4] Talya, S. S., Rajadas, J. N., and Chattopadhyay, A., 2000. "Multidisciplinary optimization for gas turbine airfoil design". *Inverse Problems in Engineering,* **8**(3), pp. 283–308.

[5] Talya, S. S., Chattopadhyay, A., and Rajadas, J. N., 2000. "An integrated multidisciplinary design optimization procedure for cooled gas turbine blades". *Collection of the 41st AIAA/ASME/ASCE/AHS/ASC Structures, Structural Dynamics, and Materials Conference and Exhibit, Vol 1 Pts 1-3*(c), pp. 1714–1726.

[6] Talya, S. S., Chattopadhyay, A., and Rajadas, J. N., 2002. "Multidisciplinary Design Optimization Procedure for Improved Design of a Cooled Gas Turbine Blade". *Engineering Optimization,* **34**(2), pp. 175–194.

[7] Mousavi, A., and Nadarajah, S. K., 2011. "Adjoint-Based Multidisciplinary Design Optimization of Cooled Gas Turbine Blades". *49th Aerospace Sciences Meeting,*(January).

[8] Song, L., Luo, C., Li, J., and Feng, Z., 2011. "Automated multi-objective and multidisciplinary design optimization of a transonic turbine stage". *Proceedings of the Institution of Mechanical Engineers, Part A: Journal of Power and Energy,* **226**(2), pp. 262–276.

[9] Chi, Z., Ren, J., and Jiang, H., 2013. "Coupled Aerothermodynamics Optimization for the Cooling System of a Turbine Vane". *Journal of Turbomachinery,* **136**(May), p. 51008.

[10] Haller, B. R., and Camus, J. J., 1984. "Aerodynamic Loss Penalty Produced by Film Cooling Transonic Turbine Blades". *Journal of Engineering for Gas Turbines and Power,* **106**(1), pp. 198–205.

[11] Tafti, D. K., and Yavuzkurt, S., 1990. "Prediction of Heat Transfer Characteristics for Discrete Hole Film Cooling for Turbine Blade Applications". *ASME Journal of Turbomachinery,* **112**(July 1990), pp. 505–511.

[12] Baldauf, S., Scheurlen, M., Schulz, a., and Wittig, S., 2002. "Correlation of Film-Cooling Effectiveness From Thermographic Measurements at Engine-like Conditions". *Journal of Turbomachinery,* **124**(4), p. 686.

[13] Bradley, A., 2009. Prediction of vane film cooling in gas turbines Correlations and Parameters. Tech. rep., Linkoping Institute of Technology, Linkoping, Sweden.

[14] Drela, M., and Youngren, H., 2008. "A User ' s Guide to MISES 2 . 63". *Changes*(February).

[15] Andrew, P. L., and Kahveci, H. S., 2007. "Validation of MISES 2-D Boundary Layer Code for High Pressure Turbine Aerodynamic Design". *ASME Conference Proceedings,* **2007**(47950), pp. 879–893.

[16] Al-Zurfi, N., and Turan, A., 2016. "LES of rotational effects on film cooling effectiveness and heat transfer coefficient in a gas turbine blade with one row of air film injection". *International Journal of Thermal Sciences,* **99**, pp. 96–112.

[17] Wang, X., Bibeau, E., and Naterer, G. F., 2007. "Experimental correlation of forced convection heat transfer from a NACA airfoil". *Experimental Thermal and Fluid Science,* **31**(8), pp. 1073–1082.

[18] Arts, T., Lambert de Rouvroit, M., and Rutherford, A. W., 1990. "Aero-thermal investigation of a highly loaded transonic linear turbine guide vane cascade". *Technical note 174*(September).

[19] Halia, E. E., Lenahan, D. T., and Thomas, T. T., 1982. Energy Efficient Engine - High Pressure Turbine Test Hardware Detiled Design Report - NASA CR-167355. Tech. rep.

[20] Timko, L. P., 1984. Energy Efficient Engine High Pressure Turbine Component Test Performance Report - NASA CR-168289.